



Synthesis, structure and coordination properties of three cyclam-based ligands bearing one scorpionate arm

Ramu Kannappan^a, Yoann Rousselin^a, Rim Zaari Jabri^{a,b}, Christine Goze^a, Stéphane Brandès^a, Roger Guilard^a, Abdellah Zrineh^b, Franck Denat^{a,*}

^a ICMUB, UMR 5260, CNRS-Univ. de Bourgogne, 9 avenue Alain Savary, 21078 Dijon Cedex, France

^b Laboratoire de Physique Générale, Université Mohamed V Agdal, Faculté des Sciences, 4 avenue Ibn Battouta, B.P. 1014 RP, Rabat, Morocco

ARTICLE INFO

Article history:

Received 8 April 2010

Received in revised form 24 March 2011

Accepted 6 April 2011

Available online 19 April 2011

Keywords:

Cyclam

N-Sulfonylacetamide

X-ray studies

Metal complexes

EPR

ABSTRACT

In this work, three new cyclam-based ligands **L**₁, **L**₂ and **L**₃ bearing *N*-sulfonylacetamide pendant arm and their Cu(II), Zn(II), Cd(II) and Pb(II) complexes were synthesized and characterized by mass spectrometry, NMR, infrared and UV–Vis spectroscopies. The ligands present an original zwitterionic form in which the nitrogen atom of the sulfonylacetamide is deprotonated and one nitrogen of the macrocycle is protonated. This observation was confirmed by X-ray crystallography. The infrared spectra of the ligands revealed very low CO vibrational band values which can be explained by the fact that the oxygen atom is involved in some hydrogen bonds. The amidate form of the sulfonylacetamide arm is maintained upon complexation. Infrared data revealed a probable different coordination mode for Pb(II) than for the other three cations. Some additional studies by UV–Vis and EPR spectroscopies were performed for the Cu(II) complexes. Finally, the geometry coordination of the Cu(II) **L**₃, Zn(II) **L**₃ and Cd(II) **L**₃ complexes in the solid state was studied by X-ray crystallography.

© 2011 Elsevier B.V. All rights reserved.

1. Introduction

1,4,8,11-Tetraazacyclotetradecane (cyclam) is one of the most extensively studied macrocyclic ligands. This macrocycle can coordinate various metal ions with large stability constants [1]. Cyclam and its derivatives have also been studied as carriers of metal ions for imaging applications [2,3] and, most recently, as anti-HIV agents [4].

In most of the cyclam complexes the metal is coordinated in a square stereochemical arrangement, in which the four nitrogen atoms of the ring are coplanar with the metal center. In this situation, the complex is highly resistant to demetallation due to the so called macrocyclic effect [5].

The affinity of the macrocycle towards a specific guest, a metallic cation in most cases, might be tuned by varying the nature, the number, and the relative positions of the pendant arms on the nitrogen atoms [6]. The addition of a coordinating pendant arm such as an amide or acid arm results in a fifth binding site that can create a square pyramidal coordination polyhedron.

It should be noted that the interaction of the metal ion with the nitrogen atom bound axially is quite labile and the pendant group can be removed from the coordination sphere on pH change [7].

This type of ligand is called scorpionate. These systems can be symbolized by a rigid ring (the tetraazamacrocycle) and a flexible part (the arm).

Here, we report the synthesis of three new ligands bearing *N*-sulfonylacetamide pendant arm and their metal complexes. The *N*-sulfonylacetamide moiety, possessing a negative charge at physiologic pH, represents an isosteric alternative to the carboxylic acid group. This offers the possibility to modulate several properties of the resulting complexes (charge, size, hydrophilicity). In this work, we considered three cyclam based macrocyclic ligands, which form a zwitterion upon addition of the *N*-sulfonylacetamide arm (Fig. 1). The crystal structures highlighting such a zwitterionic form of a sulfonamide function are reported. It has to be noted that the zwitterionic form resulting from addition of the arm to the non-substituted macrocycle **L**₁ is different than the ones obtained when starting from *trans* disubstituted cyclams **L**₂ and **L**₃.

We studied the coordination properties of these new cyclam based ligands toward Cu(II), Cd(II), Zn(II) and Pb(II). The geometry of the complexes was studied by X-ray crystallography and by EPR spectroscopy. We put forward evidence that the zwitterionic form is maintained in the metal complexes.

2. Experimental

2.1. Materials and physical measurements

The chemicals used to prepare the title compounds including CuCl₂·2H₂O, Zn(NO₃)₂·6H₂O, Cd(NO₃)₂·4H₂O, Pb(NO₃)₂ were purchased from Aldrich. Cyclam, *trans*-dimethylcyclam and *trans*-di-benzylcyclam were obtained from CheMatech[®] and used without

* Corresponding author. Tel.: +33 (0)38 039 6115; fax: +33 (0)38 039 6117.

E-mail address: Franck.Denat@u-bourgogne.fr (F. Denat).

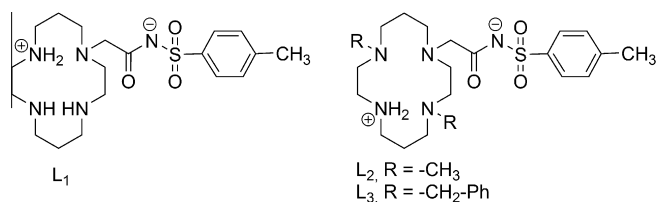


Fig. 1. Cyclam derivatives containing *N*-sulfonylacetamide arm.

further purification. 2-Bromo-*N*-tosylethanamide was prepared and purified according to the literature procedures [8]. The 1H and ^{13}C spectra were recorded at room temperature. NMR spectra were run on a BRUKER Avance 300 spectrometer at room temperature using perdeuterated solvents as internal standard. Elemental analyses were obtained on EA 1108 CHNS Fisons Instrument. Absorption spectra were recorded on a VARIAN CARY 50. Infrared spectra were recorded using a Bruker Vector 22 spectrometer ($4000\text{--}500\text{ cm}^{-1}$). Matrix-assisted laser desorption/ionization time-of-flight mass spectrometry (MALDI-TOF) was carried out using a Bruker Daltonics Proflex III spectrometer. Continuous wave (CW) EPR spectra were recorded on a Bruker ELEXSYS 500. The instrument was equipped with a 4122 SHQE/0405 X-band resonant cavity operating at 9.43 GHz, a X-band high power dual gun-oscillator bridge, and a quartz cryostat cooled with a stream of nitrogen. Sample were analyzed at 100 K in a frozen EtOH (or MeOH)/toluene mixture. The temperature was regulated with an ER 4131VT accessory. All the equipments as well as the data acquisition were controlled with the Xepr software. Spectra were recorded at 6 mW power, 100 kHz modulation, 5 G modulation amplitude and 40 ms conversion time. All the spectrometers were available at the "Plateforme d'Analyse Chimique et de Synthèse Moléculaire de l'Université de Bourgogne" (PACSMUB).

2.2. Synthesis of the ligands

2.2.1. [2'-(1,4,8,11-Tetraazacyclotetradecan-1-yl)acetyl](tosyl)amide (L_1)

To a solution of cyclam (10 g, 0.05 mol) and anhydrous potassium carbonate (1.38 g, 0.01 mol) in $CHCl_3$ (600 mL) was slowly added a solution of 2-bromo-*N*-tosylacetamide (1.45 g, 0.005 mol) in 10 mL of chloroform. The mixture was stirred for 24 h. The crude product was filtered through Celite to remove K_2CO_3 , and chloroform was evaporated. The white crude powder was dissolved in CH_3CN and cooled to $0^\circ C$ in order to precipitate the unreacted cyclam, and this operation was repeated 3–4 times until no more precipitate appeared. Recrystallization in MeOH gave pure L_1 (1.03 g, 50% yield). 1H NMR ($CDCl_3$, 300 MHz): 7.85 (d, 2H, $J = 8.2$ Hz), 7.16 (d, 2H, $J = 8.2$ Hz), 5.48 (bs, 3H), 3.05 (s, 2H), 3.00–2.53 (m, 17H), 2.34 (s, 3H), 1.81 (m, 2H), 1.67 (m, 2H). ^{13}C $\{^1H\}$ NMR ($CDCl_3$, 75.4 MHz): 177.9, 141.5, 141.2, 130.1, 128.7, 127.2, 126.9, 60.4, 54.7, 54.0, 49.8, 48.1, 47.0, 44.2, 26.5, 24.3, and 21.5. MALDI-TOF MS: $m/z = 412.35 [M]^+$. IR (ATR): $\nu(C=O)$: 1596 cm^{-1} . Anal. Calc. for $C_{19}H_{33}N_5O_3S \cdot 2MeOH$: C, 53.03; H, 8.69; N, 14.72. Found: C, 52.75; H, 8.72; N, 14.30%.

2.2.2. [2'-(4,11-Dimethyl-1,4,8,11-tetraazacyclotetradecan-1-yl)acetyl](tosyl)amide (L_2)

To a solution of *trans*-dimethylcyclam (2 g, 8.75 mmol), and anhydrous potassium carbonate (2.4 g, 17.5 mmol) in CH_3CN (300 mL) was slowly added a solution of 2-bromo-*N*-tosylacetamide (2.56 g, 8.75 mmol) in 10 mL of $CHCl_3$. The mixture was stirred for 24 h. The crude product was filtered through Celite to remove K_2CO_3 , and acetonitrile was evaporated. The white crude powder was dissolved in chloroform and cooled to $0^\circ C$ in order

to precipitate the unreacted *trans*-dimethylcyclam, and this operation was repeated 3–4 times until no more precipitate appeared. Recrystallization in hot methanol gave pure L_2 (3.3 g, 85% yield). MALDI-TOF MS: $m/z = 439.94 [M+H]^+$. 1H NMR ($CDCl_3$, 300 MHz): 7.88 (d, 2H, $J = 8.3$ Hz), 7.17 (d, 2H, $J = 8.3$ Hz), 3.45 (bs, 2H), 2.75–2.39 (m, 16H), 2.32 (s, 3H), 2.29 (s, 3H), 2.25 (s, 3H), 1.73 (m, 3H), 1.52 (m, 2H). ^{13}C $\{^1H\}$ NMR ($CDCl_3$, 75 MHz): 176.1, 139.3, 139.1, 128.5, 127.6, 126.7, 125.3, 61.3, 55.6, 53.5, 52.8, 51.4, 48.8, 46.8, 41.3, 22.2, 19.5. IR (ATR): $\nu(C=O)$: 1596 cm^{-1} . Anal. Calc. for $C_{21}H_{37}N_5O_3S \cdot 0.5CH_3OH$ (455.64): C, 56.68; H, 8.63; N, 15.37. Found: C, 57.10; H, 9.42; N, 15.20%.

2.2.3. 2'-(4,11-Dibenzyl-1,4,8,11-tetraazacyclotetradecan-1-yl)acetyl(tosyl)amide (L_3)

To a solution of *trans*-dibenzylcyclam (3.04 g, 8 mmol), and anhydrous potassium carbonate (2.07 g, 15 mmol) in CH_3CN (600 mL) was slowly added a solution of 2-bromo-*N*-tosylacetamide (2.32 g, 8 mmol) in acetonitrile (10 mL). The mixture was stirred for 24 h under argon. The crude product was filtered through Celite to remove K_2CO_3 , and acetonitrile was evaporated. The white crude powder was dissolved in chloroform and cooled to $0^\circ C$ in order to precipitate the unreacted *trans*-dibenzylcyclam, and this operation was repeated 3–4 times until no more precipitate appeared. Recrystallization in hot methanol gave pure L_3 (3.55 g, 75% yield). MALDI-TOF MS: $m/z = 592 [M+H]^+$. 1H NMR ($CDCl_3$, 300 MHz): 7.86 (d, 2H, $J = 8.5$ Hz); 7.31–7.25 (m, 10H); 7.14 (d, 2H, $J = 8.5$ Hz); 3.76 (bs, 4H); 2.91 (s, 2H); 2.89–2.36 (m, 17H); 2.31 (s, 3H); 2.15 (m, 4H); 1.71 (m, 4H). ^{13}C $\{^1H\}$ NMR ($CDCl_3$, 75 MHz): 176.8, 141.2, 140.9, 136.8, 136.6, 129.7, 129.5, 128.6, 128.4, 127.9, 127.6, 63.2, 60.4, 59.1, 55.9, 54.9, 52.4, 51.3, 50.8, 48.4, 48.3, 46.1, 23.5, 22.9, 21.4. IR (ATR): $\nu(C=O)$: 1542 cm^{-1} . Anal. Calc. for $C_{33}H_{45}N_5O_3S \cdot 0.5CH_3OH$ (607.83): C, 66.20; H, 7.79; N, 11.52. Found: C, 66.20; H, 8.64; N, 11.73%.

2.3. Synthesis of the complexes

2.3.1. General procedure

A solution of 1 equiv of the metal salt in methanol was added dropwise to a solution of ligand in methanol and the resulting mixture was refluxed for 5 h. After cooling, diethylether was added and the precipitate was filtrated.

2.3.1.1. CuL_1Cl . According to the general procedure starting from 41.4 mg (0.243 mmol) of $CuCl_2 \cdot 2H_2O$ in 10 mL of MeOH and 100 mg (0.243 mmol) of L_1 in 20 mL of MeOH. Yield: 97 mg (0.19 mmol, 79%). MALDI-TOF MS: $m/z = 473 [M-Cl]^+$. IR (ATR): $\nu(C=O)$: 1634 cm^{-1} . UV-Vis ($CHCl_3$) λ nm (ϵ , $M^{-1} cm^{-1}$) = 620 (125). Anal. Calc. for $C_{19}H_{32}ClCuN_5O_3S \cdot 0.5CH_3OH$ (525.57): C, 44.56; H, 6.52; N, 13.33. Found: C, 44.29; H, 6.79; N, 13.41%.

2.3.1.2. CuL_2Cl . According to the general procedure starting from 42.25 mg (0.248 mmol) of $CuCl_2 \cdot 2H_2O$ in 10 mL of MeOH and 102 mg (0.248 mmol) of L_2 in 20 mL of MeOH. Yield: 109 mg (0.20 mmol, 82%). MALDI-TOF MS: $m/z = 502.81 [M-Cl+H]^+$ UV-Vis ($CHCl_3$) λ nm (ϵ , $M^{-1} cm^{-1}$) = 646 (128). IR (ATR): $\nu(C=O)$: 1633 cm^{-1} . Anal. Calc. for $C_{21}H_{36}ClCuN_5O_3S \cdot 2H_2O$ (573.64): C, 43.97; H, 7.03; N, 12.21. Found: C, 43.82; H, 7.11; N, 12.33%.

2.3.1.3. CuL_3Cl . According to the general procedure starting from 144 mg (0.845 mmol) of $CuCl_2 \cdot 2H_2O$ in 20 mL of MeOH and 500 mg (0.845 mmol) of L_3 in 30 mL of MeOH. After precipitation, blue crystals of pure complex were obtained after recrystallization in CH_3OH/H_2O (394 mg, 67% yield). MALDI-TOF MS: $m/z = 654.81 [M-Cl]^+$ UV-Vis ($CHCl_3$) λ nm (ϵ , $M^{-1} cm^{-1}$) = 623 (144). IR (ATR): $\nu(C=O)$: 1578 cm^{-1} . Anal. Calc. for $C_{33}H_{44}ClCu$

$\text{N}_5\text{O}_3\text{S}\cdot 2\text{H}_2\text{O}\cdot 1.5\text{CH}_3\text{OH}$ (773.89): C, 53.54; H, 7.03; N, 9.05. Found: C, 53.40; H, 7.04; N, 9.37%.

2.3.1.4. ZnL_1NO_3 . According to the general procedure starting from 74.52 mg (0.243 mmol) of $\text{Zn}(\text{NO}_3)_2\cdot 6\text{H}_2\text{O}$ in 15 mL of MeOH and 100 mg (0.243 mmol) of L_1 in 20 mL of MeOH. After filtration, the solid was further washed with dichloromethane. Yield: 99 mg (0.185 mmol, 76%). MALDI-TOF MS: $m/z = 474$ $[\text{M}-\text{NO}_3]^+$. IR (ATR): $\nu(\text{C}=\text{O})$: 1650 cm^{-1} . Anal. Calc. for $\text{C}_{19}\text{H}_{32}\text{N}_6\text{O}_6\text{SZn}\cdot 2\text{H}_2\text{O}$: C, 39.76; H, 6.32; N, 14.64. Found: C, 39.65; H, 6.45; N, 14.70%.

2.3.1.5. ZnL_2NO_3 . According to the general procedure starting from 67.72 mg (0.228 mmol) of $\text{Zn}(\text{NO}_3)_2\cdot 6\text{H}_2\text{O}$ in 15 mL of MeOH and 100 mg (0.228 mmol) of L_2 in 20 mL of MeOH. After filtration, further recrystallization in hot CH_3OH gave pure complex (102 mg, 79% yield). MALDI-TOF MS: $m/z = 504.67$ $[\text{M}-\text{NO}_3]^+$. IR (ATR): $\nu(\text{C}=\text{O})$: 1618 cm^{-1} . Anal. Calc. for $\text{C}_{21}\text{H}_{36}\text{N}_6\text{O}_6\text{SZn}$: C, 44.56; H, 6.41; N, 14.85. Found: C, 44.49; H, 6.50; N, 14.88%.

2.3.1.6. ZnL_3NO_3 . According to the general procedure starting from 251 mg (0.845 mmol) of $\text{Zn}(\text{NO}_3)_2\cdot 6\text{H}_2\text{O}$ in 20 mL of MeOH and 500 mg (0.845 mmol) of L_3 in 30 mL of MeOH. The solution was refluxed during 5 h, then the crystals were obtained after evaporation of the solvent. After filtration, further recrystallization in hot CH_3OH gave pure complex. Yield: 491 mg (0.201 mmol, 81% yield). MALDI-TOF MS: $m/z = 654.10$ $[\text{M}-\text{NO}_3]^+$. IR (ATR): $\nu(\text{C}=\text{O})$: 1562 cm^{-1} . Anal. Calc. for $\text{C}_{33}\text{H}_{44}\text{N}_6\text{O}_6\text{SZn}\cdot 0.5\text{CH}_3\text{OH}$: C, 54.80; H, 6.31; N, 11.45. Found: C, 55.01; H, 6.91; N, 11.69%.

2.3.1.7. CdL_1NO_3 . According to the general procedure starting from 75 mg (0.243 mmol) of $\text{Cd}(\text{NO}_3)_2\cdot 4\text{H}_2\text{O}$ in 15 mL of MeOH and 100 mg (0.243 mmol) of L_1 in 20 mL of MeOH. After filtration, the complex was further recrystallized in hot CH_3OH . Yield: 97 mg (0.165 mmol, 68%). MALDI-TOF MS: $m/z = 521.1$ $[\text{M}-\text{NO}_3]^+$. IR (ATR): $\nu(\text{C}=\text{O})$: 1619 cm^{-1} . Anal. Calc. for $\text{C}_{19}\text{H}_{32}\text{CdN}_6\text{O}_6\text{S}\cdot 0.5\text{CH}_3\text{OH}$: C, 39.01; H, 5.51; N, 14.37. Found: C, 38.95; H, 5.58; N, 14.42%.

2.3.1.8. CdL_2NO_3 . According to the general procedure starting from 177 mg (0.569 mmol) of $\text{Cd}(\text{NO}_3)_2\cdot 4\text{H}_2\text{O}$ in 20 mL of MeOH and 250 mg (0.569 mmol) of L_2 in 25 mL of MeOH. After filtration, the complex was further recrystallized in hot CH_3OH . Yield: 227 mg (0.37 mmol, 65%). MALDI-TOF MS: $m/z = 551.67$ $[\text{M}-\text{NO}_3]^+$. IR (ATR): $\nu(\text{C}=\text{O})$: 1648 cm^{-1} . Anal. Calc. for $\text{C}_{21}\text{H}_{36}\text{CdN}_6\text{O}_6\text{S}\cdot 0.5\text{CH}_3\text{OH}$: C, 41.05; H, 6.09; N, 13.36. Found: C, 40.95; H, 6.17; N, 13.38%.

2.3.1.9. CdL_3NO_3 . According to the general procedure starting from 260 mg (0.845 mmol) of $\text{Cd}(\text{NO}_3)_2\cdot 4\text{H}_2\text{O}$ in 25 mL of MeOH and 500 mg (0.845 mmol) of L_3 in 30 mL of MeOH. After refluxing during 5 h, and slow evaporation of the solvent, colorless crystals of pure complex were obtained. Yield: 398 mg (0.52 mmol, 62%). MALDI-TOF MS: $m/z = 703.73$ $[\text{M}-\text{NO}_3]^+$. IR (ATR): $\nu(\text{C}=\text{O})$: 1685 cm^{-1} . Anal. Calc. for $\text{C}_{33}\text{H}_{44}\text{CdN}_6\text{O}_6\text{S}$ (765.22): C, 51.80; H, 5.80; N, 10.98. Found: C, 51.74; H, 5.84; N, 11.00%.

2.3.1.10. PbL_1NO_3 . According to the general procedure starting from 81 mg (0.243 mmol) of $\text{Pb}(\text{NO}_3)_2$ dissolved in 20 mL of H_2O and 100 mg (0.243 mmol) of L_1 in 20 mL of H_2O . After filtration, the product was further washed with a mixture of methanol/water. Yield: 10 mg (0.13 mmol, 52%). MALDI-TOF MS: $m/z = 618$ $[\text{M}-\text{NO}_3]^+$. IR (ATR): $\nu(\text{C}=\text{O})$: 1596 cm^{-1} . Anal. Calc. for $\text{C}_{19}\text{H}_{32}\text{N}_6\text{O}_6\text{PbS}\cdot 2\text{H}_2\text{O}$ (715.79): C, 31.88; H, 5.07; N, 11.74. Found: C, 31.65; H, 5.15; N, 11.87%.

2.3.1.11. PbL_2NO_3 . According to the general procedure starting from 75.51 mg (0.228 mmol) of $\text{Pb}(\text{NO}_3)_2$ dissolved in 20 mL of H_2O and 100 mg (0.228 mmol) of L_2 in 20 mL of H_2O . After filtration, the product was further washed with a mixture of methanol/water. Yield: 10 mg (0.14 mmol, 60%). MALDI-TOF MS: $m/z = 646$ $[\text{M}-\text{NO}_3]^+$. IR (ATR): $\nu(\text{C}=\text{O})$: 1596 cm^{-1} . Anal. Calc. for $\text{C}_{21}\text{H}_{36}\text{N}_6\text{O}_6\text{PbS}\cdot 2\text{H}_2\text{O}$ (743.84): C, 33.91; H, 5.42; N, 11.30. Found: C, 33.82; H, 5.51; N, 11.33%.

2.3.1.12. PbL_3NO_3 . According to the general procedure starting from 280 mg (0.845 mmol) of $\text{Pb}(\text{NO}_3)_2$ dissolved in 30 mL of H_2O and 500 mg (0.845 mmol) of L_3 in 70 mL of H_2O . After filtration, the product was further washed with a mixture of methanol/water. Yield: 421 mg (0.59 mmol, 58%). MALDI-TOF MS: $m/z = 798.87$ $[\text{M}-\text{NO}_3]^+$. IR (ATR): $\nu(\text{C}=\text{O})$: 1542 cm^{-1} . Anal. Calc. for $\text{C}_{33}\text{H}_{44}\text{N}_6\text{O}_6\text{PbS}\cdot \text{H}_2\text{O}$ (878.02): C, 45.14; H, 5.28; N, 9.57. Found: C, 45.08; H, 5.32; N, 9.60%.

2.4. X-ray crystallography

Experimental details of the X-ray analyses are provided in Table 1 for ligand L_1 and L_3 and Table 2 for the L_3 complexes. Diffraction data were collected on a Nonius Kappa CCD or Nonius Kappa Apex II diffractometer equipped with a nitrogen jet stream low-temperature system (Oxford Cryosystems). The X-ray source was graphite-monochromated Mo $K\alpha$ radiation ($\lambda = 0.71073\text{ \AA}$) from a sealed tube. In both cases, lattice parameters were obtained by least-squares fit to the optimized setting angles of the entire set of collected reflections. No temperature drift was observed during the data collections. Data were reduced by using DENZO software [9] without applying absorption corrections; the missing absorption corrections were partially compensated by the data scaling procedure. The structures were solved by direct methods using the SIR92 [10] program. Refinements were carried out by full-matrix least-squares on F^2 using the SHELXL97 [11] program and the complete set of reflections. Anisotropic thermal parameters were used for non-hydrogen atoms. All H atoms, on carbon atom, were placed at calculated positions using a riding model with $C-H = 0.95\text{ \AA}$ (aromatic), 0.98 \AA (methyl), 0.99 \AA (methylene) or 1 \AA (methine) with $U_{\text{iso}}(\text{H}) = 1.5 U_{\text{eq}}(\text{CH}_3)$, $U_{\text{iso}}(\text{H}) = 1.2 U_{\text{eq}}(\text{CH}_2)$ or $U_{\text{iso}}(\text{H}) = 1.2 U_{\text{eq}}(\text{CH})$. H atoms on nitrogen atoms were located in

Table 1
Crystallographic data for ligands L_1 and L_3 .

Ligands	L_1	L_3
Formula	$\text{C}_{26}\text{H}_{42}\text{N}_6\text{O}_5\text{S}_2$	$\text{C}_{33}\text{H}_{45}\text{N}_6\text{O}_5\text{S}$
Formula weight	582.78	591.80
Crystal system	monoclinic	monoclinic
Space group	$P21/c$	$P21/c$
Color	colorless	colorless
Crystal size (mm)	$0.12 \times 0.12 \times 0.10$	$0.55 \times 0.17 \times 0.12$
<i>Unit cell dimensions</i>		
a (Å)	15.3876(4)	11.8976(2)
b (Å)	9.3581(4)	19.2804(4)
c (Å)	20.5995(7)	16.2070(3)
α (°)	90	90
β (°)	96.683(2)	123.135(1)
γ (°)	90	90
V (Å ³)	2946.15(18)	3113.17(10)
Z	4	4
D_{calc} (mg m ⁻³)	1.314	1.263
T (K)	115(2)	115(2)
Number of reflections	8800	13 962
θ (°)	1.33–27.50	2.94–27.49
μ (mm ⁻¹)	0.227	0.146
$F(0\ 0\ 0)$	1248	1272
R_1, wR_2 [$I > 2\sigma(I)$]	0.0741, 0.1340	0.0388, 0.0879
Goodness-of-fit (GOF) on F^2	1.129	1.022

Table 2
Crystallographic data for complexes of **L**₃.

Ligands	CdL ₃ NO ₃	ZnL ₃ NO ₃	CuL ₃ Cl
Formula	C ₃₃ H ₄₄ CdN ₆ O ₆ S	C ₃₃ H ₄₄ N ₆ O ₆ SZn	C ₃₄ H ₆₀ ClCuN ₅ O ₁₀ S
Formula weight	765.20	718.17	829.92
Crystal system	triclinic	monoclinic	orthorhombic
Space group	<i>P</i> $\bar{1}$	<i>P</i> 21	<i>Pbca</i>
Color	colorless	colorless	blue
Crystal size (mm)	0.12 × 0.12 × 0.10	0.55 × 0.17 × 0.12	0.17 × 0.12 × 0.08
<i>Unit cell dimensions</i>			
<i>a</i> (Å)	9.9591(2)	10.2459(4)	10.2100(2)
<i>b</i> (Å)	11.3696(4)	14.7449(5)	25.8373(6)
<i>c</i> (Å)	15.6131(5)	11.1222(4)	30.7536(7)
α (°)	74.590(1)	90	90
β (°)	86.748(2)	105.568(2)	90
γ (°)	77.240(2)	90	90
<i>V</i> (Å ³)	1662.24(9)	1618.64(10)	8112.8(3)
<i>Z</i>	2	2	8
<i>D</i> _{calc} (mg m ⁻³)	1.529	1.474	1.359
<i>T</i> (K)	115(2)	115(2)	115(2)
Number of reflections	14 404	6652	17 642
θ (°)	2.03–27.55	1.90–27.48	1.71–27.49
μ (mm ⁻¹)	0.774	0.879	0.714
<i>F</i> (0 0 0)	792	756	3528
<i>R</i> ₁ , <i>wR</i> ₂	0.0378, 0.0745	0.0460, 0.0950	0.0595, 0.1218
[<i>I</i> > 2 σ (<i>I</i>)]			
Goodness-of-fit (GOF) on <i>F</i> ²	1.097	1.108	1.130

the Fourier difference maps. Their position parameters were refined freely with $U_{\text{iso}}(\text{H}) = 1.2 U_{\text{eq}}(\text{N})$. In CdL₃NO₃, oxygen atoms on the disordered nitrate anion (45/55) were constrained with EADP instructions to maintain a reasonable model. Finally, H atoms on water molecule in CuL₃Cl were located in the Fourier difference maps. Their position parameters were fixed.

3. Results and discussion

3.1. Synthesis of the ligands

Ligand **L**₁ was synthesized by reacting 10 equiv of cyclam and 1 equiv of 2-bromo-*N*-tosylethanamide in a low dissociating solvent in order to favor the monofunctionalization of the macrocycle (Scheme 1)[12]. The excess of unreacted cyclam was eliminated by precipitation in cold acetonitrile.

Interestingly, proton NMR analysis displays the disappearance of the amide proton on the sulfonamide group. Elemental analysis and X-ray diffraction confirm this observation. These analyses reveal a zwitterionic neutral system containing an amidate form on the sulfonamide group and a protonated nitrogen atom. Specifically, the proton is located on the nitrogen atom which is separated from the nitrogen bearing the arm by a propyl group. The localization of the proton on this nitrogen can be explained by a favorable intramolecular hydrogen bond between this proton and the

oxygen atom of the carbonyl group of the sulfonylacetamide arm (Fig. 2).

Ligands **L**₂ and **L**₃ were obtained by equimolar addition of 2-bromo-*N*-tosylethanamide and 1,8-dimethylcyclam or 1,8-dibenzylcyclam in refluxing acetonitrile (Scheme 2). They were isolated in 87% and 70% yield, respectively.

¹H NMR shows that the two ligands contain an amidate group, as observed for **L**₁. These amidate forms were confirmed by X-ray analyses. However the zwitterionic form in these two ligands is different from **L**₁. Indeed, the protonated nitrogen is localized on the opposite of the sulfonylacetamide arm. This difference can be explained by the presence of methyl or benzyl groups on the two nitrogen atoms adjacent to the arm in **L**₂ and **L**₃. The remaining secondary amine group is more basic than the three substituted tertiary amine groups.

3.2. Structures of **L**₁ and **L**₃

Some prismatic colorless crystals of **L**₁ and **L**₃ were obtained by slow evaporation of MeOH. The compound **L**₁ co-crystallized with tosylamine, which was formed during recrystallization. **L**₁ and **L**₃ adopt a zwitterionic form resulting from the proton transfer of the sulfonamide to the nitrogen atom of the macrocyclic ring. This zwitterionic form does not involve the same nitrogen atom in **L**₁ and in **L**₃ and so it gives rise to different intermolecular and intramolecular interactions in the two ligands. Similar zwitterionic forms have been already reported in the literature [13].

In the ligand **L**₁, the protons on the nitrogen atom N4 interact with the nitrogen atom N1 of the macrocyclic ring, the oxygen atom of the pendant arm and an oxygen atom of the sulfonamide group from another asymmetric unit. The ORTEP [14] view of inter- and intramolecular hydrogen bonds is depicted in Fig. 2. We can also notice that the proton H31 on N3 points toward the tosylamide phenyl group. The distance and angle between hydrogen H31 and the centroid Ct of the phenyl group reveal a weak interaction ($d(\text{N}3 \dots \text{Ct}) = 3.471(1) \text{ \AA}$ and $\text{N}3\text{--H}31\text{--Ct} = 154(3)^\circ$) [15].

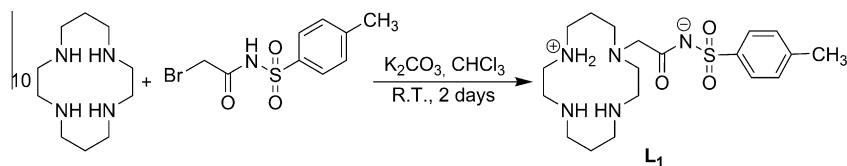
The delocalization of the lone pair of the nitrogen atom can be confirmed by infrared spectroscopy. Indeed, the C=O band appears at 1704 cm⁻¹ in bromo-*N*-tosylethanamide while this value is considerably lowered to 1596 and 1542 cm⁻¹ in **L**₁ and **L**₃, respectively.

The X-ray structure of **L**₃ reveals intramolecular hydrogen bonding between a proton on N3 and nitrogen atoms N1 and N2, as well as intermolecular hydrogen bonding with the oxygen atom O3 from the amide group of another asymmetric unit (Fig. 3).

The C–O bond in **L**₃ (1.2519(18) Å) is longer than in **L**₁ (1.238(4) Å) because the intermolecular hydrogen bond between the oxygen atom O3 and N3–H of another asymmetric unit (N3–H...O3 = 2.7085(16) Å) is shorter in **L**₃, and thus stronger than the intramolecular hydrogen bond between the oxygen atom O3 and N3–H in **L**₁ (N4–H...O3 = 2.863(4) Å). This is also consistent with infrared data (**L**₁: $\nu(\text{CO}) = 1596 \text{ cm}^{-1}$, **L**₃: $\nu(\text{CO}) = 1542 \text{ cm}^{-1}$).

3.3. Synthesis of the complexes

The Cu(II), Zn(II), Cd(II) and Pb(II) complexes were prepared by reaction of the ligands **L**₁–**L**₃ with CuCl₂·2H₂O, Zn(NO₃)₂·6H₂O,



Scheme 1. Synthesis of **L**₁.

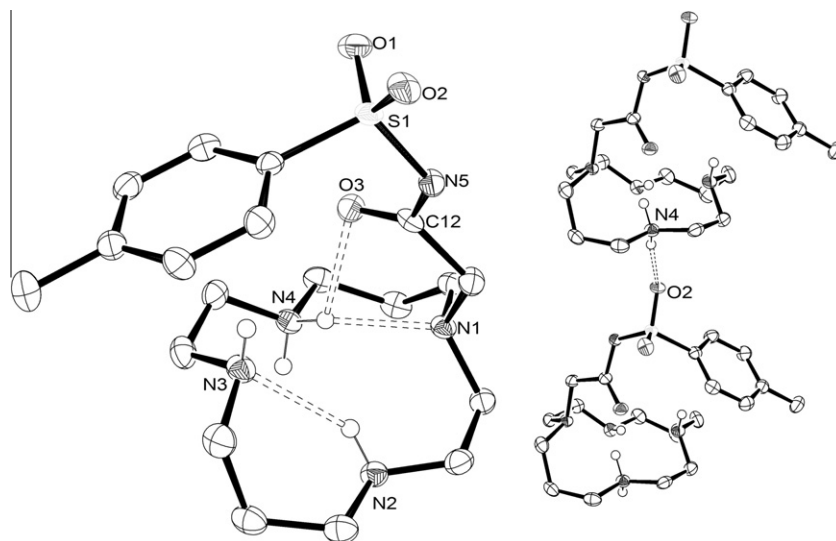
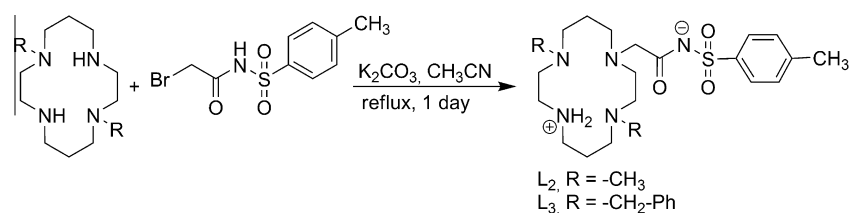


Fig. 2. ORTEP [14] view of L_1 . The thermal ellipsoids are at the 50% probability level. H-atoms attached to carbon are omitted for clarity. Tosylamine which co-crystallized with L_1 is not depicted. Intramolecular (left) and intermolecular (right) hydrogen bonds are indicated by dashed lines. The D–H...A distances are N2H–N3 = 2.996(4) Å, N4H–N1 = 2.867(4) Å, N4H–O3 = 2.863(4) Å, N4H–O2 = 2.754(4) Å.



Scheme 2. Synthesis of L_2 and L_3 .

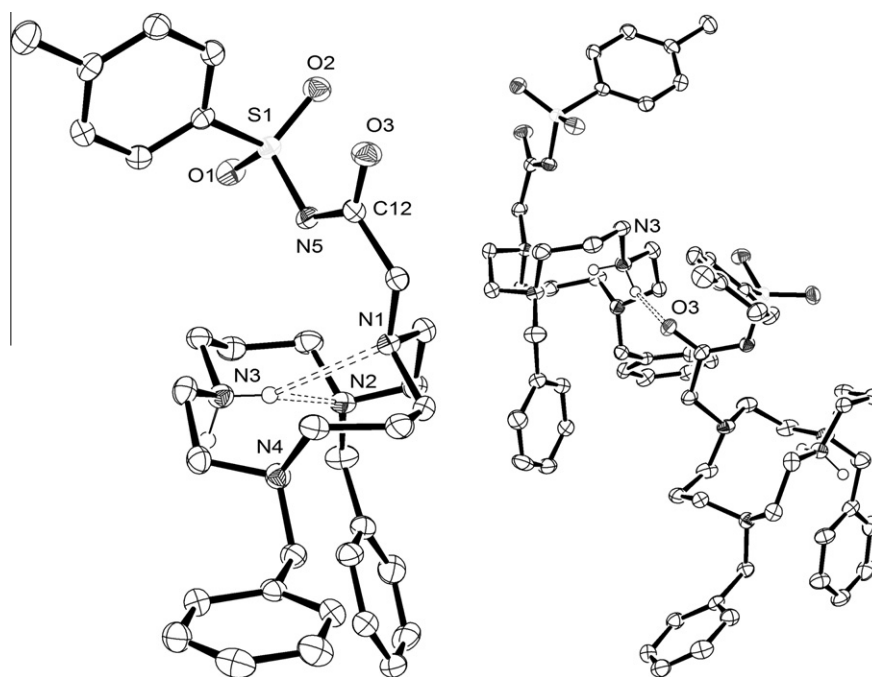


Fig. 3. ORTEP [14] drawing of L_3 ligand. The thermal ellipsoids are at the 50% probability level. H-atoms attached to carbon are omitted for clarity. Intermolecular (left) and intramolecular (right) hydrogen bonds are indicated by dashed lines. The D–H...A distances are N3H–N2 = 2.9047(17) Å, N3H–N1 = 3.4373(17) Å, N3H–O3 = 2.7085(16) Å.

$Cd(NO_3)_2 \cdot 4H_2O$ and $Pb(NO_3)_2$, respectively. They were characterized by elemental analysis, mass spectrometry, UV–Vis, IR and

EPR spectroscopy, and the solid-state structures of CuL_3Cl , ZnL_3NO_3 , CdL_3NO_3 were determined by X-ray diffraction analysis.

This solid-state analysis shows that the amidate form was maintained upon complexation. Moreover, in the three structures, the carbonyl group of the tosylacetamide arm is coordinated to the metal cation (Figs. 4, 6 and 7).

Infrared spectra shown that the metallation of L_3 with Cu(II), Zn(II) and Cd(II) induced a shift of the CO band from 1542 to 1562–1578 cm^{-1} . This shift can be explained by the fact that after coordination O3 atom is not involved in hydrogen bonding. The same phenomenon was observed with the ligands L_1 and L_2 . We can deduce from these observations that the carbonyl group probably coordinates to Cu(II), Zn(II) and Cd(II) in the three ligands L_1 – L_3 . Concerning Pb(II) cation, no shift of the vibration band of the CO bond was observed upon complexation with ligands L_1 – L_3 , suggesting that the pendant arm in these complexes is not involved in the coordination of Pb(II).

3.4. Structures of $\text{Cd}L_3\text{NO}_3$, $\text{Zn}L_3\text{NO}_3$ and $\text{Cu}L_3\text{Cl}$

The crystal structures of the three complexes of L_3 with Cd^{2+} , Zn^{2+} and Cu^{2+} have been obtained, and the amidate form was observed in three cases. The coordination geometry of the metal, the conformation of the macrocycle and some selected bond lengths are reported in Table 3.

The cadmium complex adopts a *cis* I conformation (see Fig. 4) [16].

The asymmetric unit contains one molecule with a coordinated nitrate counter ion disordered over two sites (55:45). The Cd(II) is hexacoordinated by four non-coplanar nitrogen atoms of the macrocycle, one oxygen from the nitrate counter ion and the oxygen of the carbonyl group on the pendant arm. The Cd–N distances range from 2.304(2) to 2.367(2) Å, while the Cd–O bond lengths are 2.267(2) to 2.406(5) Å, which is in good agreement with the distances found in the literature (2.332(88) and 2.412(226) for Cd–N and Cd–O, respectively) [17]. The different distances and angles revealed an octahedral distorted geometry (see Table 3). One may notice the hydrogen bonding interactions between the hydrogen atoms attached to N3 and the oxygen of the nitrate counter ion (Fig. 5).

The Zn(II) complex of the dibenzyl derivative L_3 , adopts a *trans* III arrangement (see Fig. 6). The Zn(II) is hexacoordinated by four

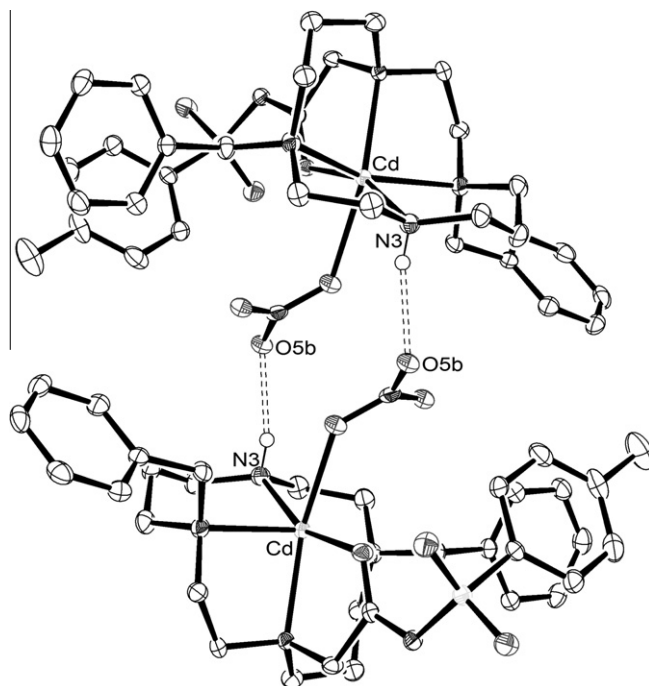


Fig. 5. ORTEP [14] view of H-bonds in $\text{Cd}L_3\text{NO}_3$ complex. The thermal ellipsoids are at the 50% probability level. H-atoms attached to carbon and disordered parts are omitted for clarity. The D–H...A distance is $\text{N3H}\cdots\text{O5b} = 2.861(7)$ Å. Intermolecular hydrogen bonds are indicated by dashed lines.

coplanar nitrogen atoms of the macrocycle and two oxygen atoms in apical position, one from the nitrate counter ion, one from the carbonyl group in the pendant arm.

The regular octahedral coordination sphere of Zn(II) is confirmed by the N–Zn–N angles (cf. Table 4) close to 90° and by the Zn–N distances ranging from 2.054(3) to 2.237(3) Å, while the Zn–O bond lengths are 2.131(3) and 2.229(3) Å. These values are in good agreement with the distances found in the literature (2.196(195) and 2.116(111) Å for Zn–N and Zn–O, respectively

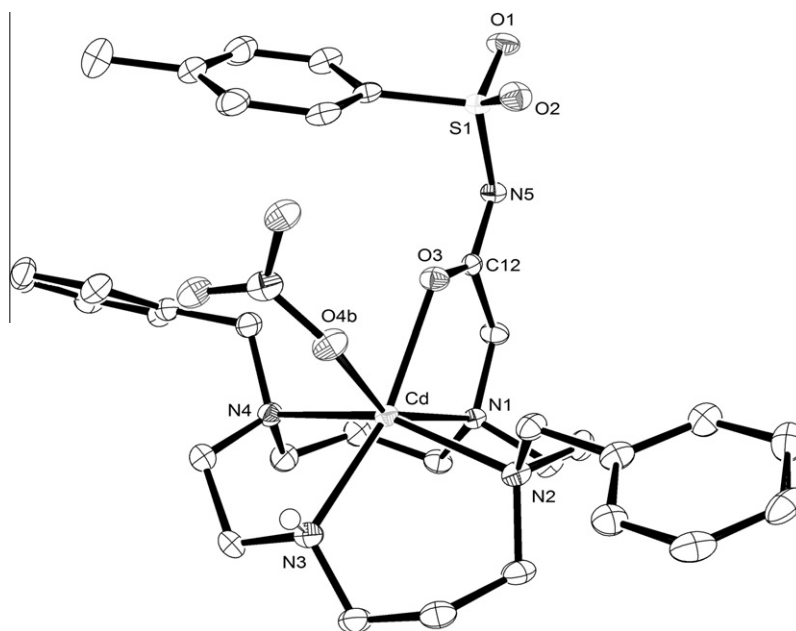


Fig. 4. ORTEP [14] view of *cis* I $\text{Cd}L_3\text{NO}_3$ complex. The thermal ellipsoids are at the 50% probability level. H-atoms attached to carbon and disordered parts are omitted for clarity.

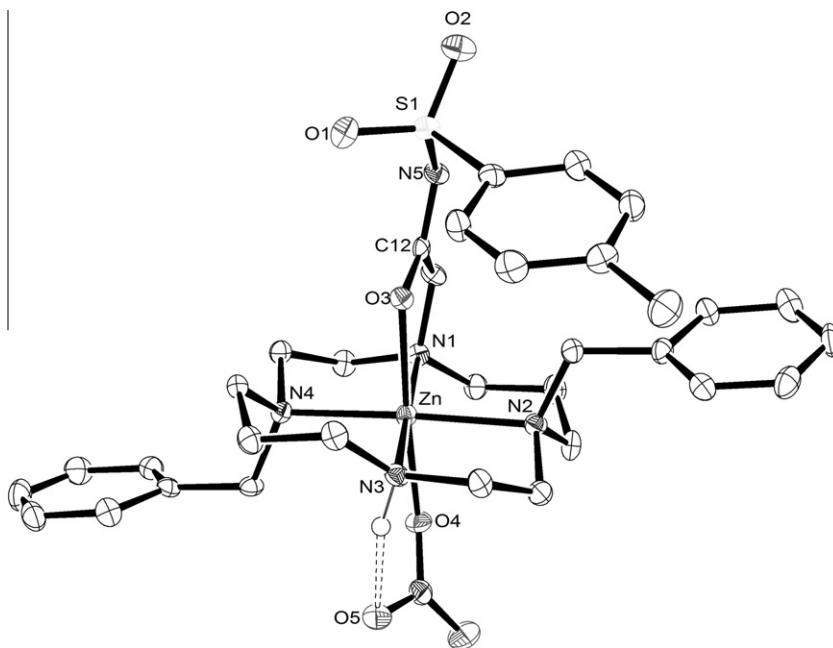


Fig. 6. ORTEP [14] view of *trans* III ZnL_3NO_3 complex. The thermal ellipsoids are at the 50% probability level. H-atoms attached to carbon are omitted for clarity. Dashed lines indicate intramolecular hydrogen bonds. $\text{N3-H}\cdots\text{O5} = 2.967(5)$ Å.

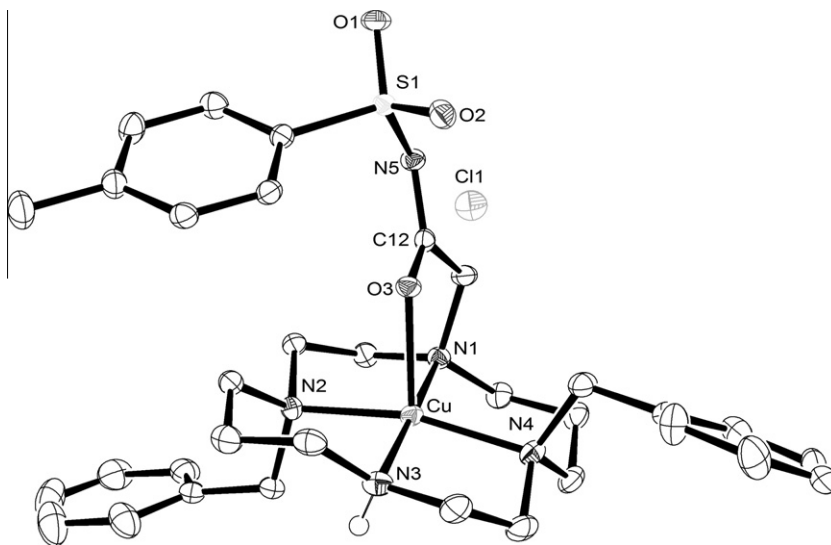


Fig. 7. ORTEP [14] view of *trans* III CuL_3Cl complex. The thermal ellipsoids are at the 50% probability level. H-atoms attached to carbon and solvent molecules are omitted for clarity.

Table 3
Coordination geometry, conformation and selected bond lengths [Å] for CdL_3NO_3 , ZnL_3NO_3 and CuL_3Cl .

Metal	Cd^{2+}	Zn^{2+}	Cu^{2+}
Geometry	distorted octahedron	octahedron	square pyramid
Symmetry	O_h	O_h	C_{4v}
Conformation	<i>cis</i> I	<i>trans</i> III	<i>trans</i> III
N1–M	2.367(2)	2.117(3)	2.065(3)
N2–M	2.365(2)	2.237(3)	2.084(3)
N3–M	2.304(2)	2.054(3)	1.992(3)
N4–M	2.358(2)	2.198(3)	2.089(3)
O3–M	2.267(2)	2.131(3)	2.204(2)
O4B–M	2.406(5)	2.229(3)	
O4A–M	2.329(7)		

[18]). It is interesting to note that the Zn–N3 bond length (2.054(3) Å) is somewhat shorter than the other Zn–N distances. This is probably due to a hydrogen bonding interaction between the hydrogen atom attached to N3 and the oxygen atom O5 from the nitrate counter ion.

The complex CuL_3NO_3 also adopts a *trans* III arrangement (Fig. 7). The asymmetric unit of the Cu(II) complex of **5** contains the Cu(II) complex, a non-coordinated chloride counter ion, six water molecules and one methanol molecule.

Cu(II) is pentacoordinated by four coplanar nitrogen atoms from the macrocycle and one oxygen atom in apical position belonging to the carbonyl group of the pendant arm. The regular pyramidal coordination sphere of Cu^{2+} is confirmed by the N–Cu–N angles

Table 4
Selected angles [°] in the complexes CdL_3NO_3 , ZnL_3NO_3 and CuL_3Cl .

Angle (°)	CdL_3NO_3	ZnL_3NO_3	CuL_3Cl
N1–M–N2	79.67(8)	93.26(12)	86.33(10)
N2–M–N3	89.71(8)	85.16(12)	90.74(11)
N3–M–N4	78.40(8)	94.78(12)	85.82(11)
N4–M–N1	89.98(8)	86.92(12)	95.95(10)
O3–M–N1	75.41(7)	81.23(11)	82.62(9)
O3–M–N2	96.32(8)	92.77(12)	91.86(9)
N4–M–O4B	103.04(12)	91.66(12)	
N4–M–O4A	93.05(15)		

(Table 4) close to 90° and the Cu–N distance ranging from 1.992(3) to 2.089(3) Å, while the Cu–O bond length is 2.204(3) Å. These distances are in good agreement with those of analogous systems [19]. It is interesting to note that the N–Cu bond lengths are somewhat shorter than the Cu–O bond length. This deformation is related to the d^9 copper(II) electronic configuration and reflects an energy stabilization of the complex by lowering of symmetry (“Jahn–Teller” effect). There are also some hydrogen bonding interactions between the hydrogen atom attached to N3 and the oxygen atom from a water molecule.

3.5. UV–Vis spectral properties and EPR studies of Cu complexes

The UV–Vis spectra of the three Cu(II) complexes were recorded in CHCl_3 . These complexes exhibit a d–d [20] transition band with $\lambda_{\text{max}} = 620 \text{ nm}$ ($\epsilon = 125 \text{ M}^{-1} \text{ cm}^{-1}$) for L_1 , 648 nm ($\epsilon = 128 \text{ M}^{-1} \text{ cm}^{-1}$) for L_2 and 623 nm ($\epsilon = 144 \text{ M}^{-1} \text{ cm}^{-1}$) for L_3 . These λ_{max} values are consistent with a pentacoordinated center in a square pyramidal geometry, or an hexacoordinated center with an octahedral geometry.

Electron paramagnetic resonance corroborates the coordination geometry proposed for the copper ion in Cu(II) complexes. EPR spectra were recorded in EtOH (or MeOH)/toluene 3/1 solution at 100 K for the three $\text{CuL}_{1-3}\text{Cl}$ complexes (Fig. 8). The spectra are characterized by a magnetic anisotropy in frozen solution and exhibit the three x, y and z contributions for Cu(II) complexes typical of the $S = 1/2$ state with slight rhombic distortions.

The spectra show the typical four line pattern in the lower field part of the spectra as expected from the coupling of the unpaired electron with the nuclear spin ($I = 3/2$) of the copper(II) nucleus [21]. The EPR parameters reported in Table 5 follow the sequence $g_3 (\sim 2.20) > g_2 (\sim 2.08) \sim g_1 (\sim 2.05) > g_e (2.0023)$, which indicates that the magnetic orbital in the ground state corresponds to $d_{x^2-y^2}$, as expected for a nearly axial g tensor with small rhombic distortions [22]. These results are consistent with copper(II) complexes in an axial symmetry, namely a tetragonal geometry around the Cu(II) center, with a square pyramidal arrangement with slight equatorial distortions or Jahn–Teller axially elongated octahedral geometry. Moreover, the g_i and the A_z hyperfine coupling constants values are in good agreement with those found for copper complexes of N-functionalized cyclams [23].

The three complexes appear to have similar symmetry by considering the rhombicity factor R (Table 5), which is a good indicator of the geometry, values less than 1 being typical of C_{4v} or D_{4h} tetragonal geometry. According to the ligand field theory, an increasing g_z value is concomitant to the decrease of the A_z value as the equatorial ligand field becomes weaker or as the axial ligand field becomes stronger due to a less overlap of the $d_{x^2-y^2}$ magnetic orbital with the nitrogen atom orbitals of the ligand [24]. Thus, it is possible to get more structural information from the EPR data by considering the g_z/A_z ratio, which can be used as an estimate of the coordination geometry. Values of 110–120 cm have been assigned to planar or axially elongated octahedral complexes, while

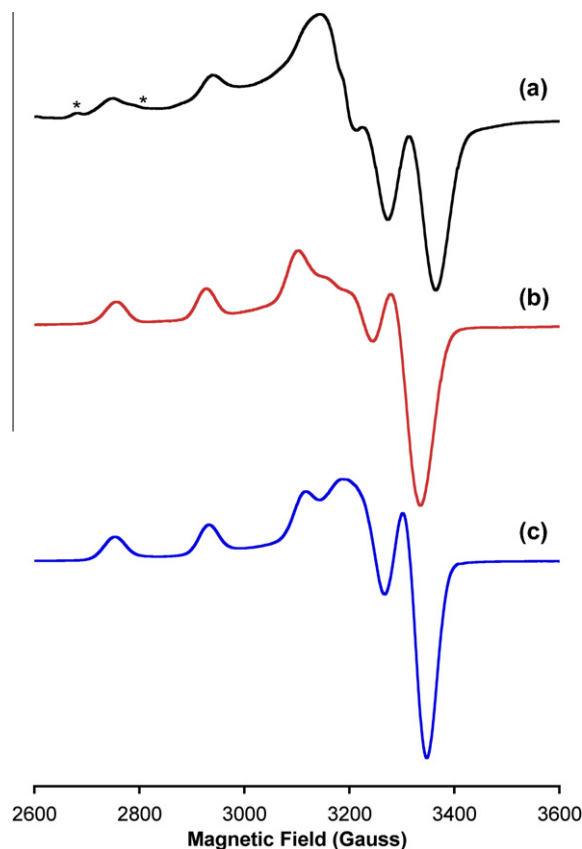


Fig. 8. X-band EPR spectra ($\nu = 9.309 \text{ GHz}$) recorded at 100 K in EtOH (or MeOH for CuL_3Cl)/toluene (3/1 v/v) solution for (a) CuL_1Cl , (b) CuL_2Cl and (c) CuL_3Cl . The asterisk indicates the presence of an impurity in the CuL_1Cl spectrum.

Table 5

EPR data for $\text{CuL}_{1-3}\text{Cl}$ complexes recorded at 100 K in EtOH (or MeOH for CuL_3Cl)/toluene (3/1 v/v) frozen solution.

Compounds	g_3 ($= g_z$)	g_1, g_2^a	Rhombicity ^a	$A_z \times 10^{-4}$ (cm^{-1})	g_z/A_z (cm)
CuL_1Cl	2.188	2.082 2.046	0.34	191	114
CuL_2Cl	2.201	2.094 2.062	0.30	179	123
CuL_3Cl	2.194	2.075 2.050	0.21	186	118

^a The rhombicity of the complex gives $g_x \neq g_y$ ($g_{\perp} = g_x = g_y$ for complexes with a four order symmetry axis). The rhombicity factor [26] is defined by $R = (g_2 - g_1)/(g_3 - g_2)$ with $g_3 > g_2 > g_1$.

values in the 120–150 cm range are typical for square pyramidal complexes exhibiting slight to moderate distortions. Higher values are indicative of considerable distortions. The A_z and g_z/A_z values indicate slight differences between the three $\text{CuL}_{1-3}\text{Cl}$ complexes, and the values of $191 \times 10^{-4} \text{ cm}^{-1}$ and 114 cm, respectively, for CuL_1Cl are characteristic of an axially elongated octahedral coordination geometry with almost no in plane distortion and a weak axial ligand field strength. Considering the more σ -bond donor of the secondary amine compared to tertiary amine, L_1 behaves as a stronger ligand field chelate than L_2 and L_3 , which explains the slightly higher A_z value and lower g_z/A_z ratio observed for CuL_1Cl . The values reported for CuL_3Cl are also consistent with a pentacoordinated or a hexacoordinated Cu(II) complex with a strong equatorial ligand field, that is a short in plane Cu–N bond and a longer axial Cu–O bonds. Given that L_1 and L_3 are pentadentate, the

hypothesized octahedral environment is certainly due to axial coordination of a solvent molecule (EtOH) at the opposite side of oxygen atom from the amide group. Finally, CuL₂Cl complex shows a slightly more distorted environment around Cu(II), as reflected by the A_z and g_z/A_z values.

For pentacoordinated complexes, efforts have been made to obtain quantitative measurements of distortions, the simplest angular parameter commonly used for these complexes is that proposed by Addison [25]. A τ value is calculated according to Eq. (1), where α and β describe the two largest L–M–L bond angles, so that complexes with an ideal trigonal bipyramidal structure have $\tau = 1$, and those with ideal square pyramidal geometry have $\tau = 0$, and distorted complexes give τ values between 0 and 1:

$$\tau = (\alpha - \beta)/60 \quad (1)$$

A value of 0.15 calculated for CuL₃Cl thanks to its crystallographic data indicates an almost ideal square pyramidal geometry with a copper ion lying in the mean plane of the four nitrogen atoms, thus leading to a strong overlap of the metal $d_{x^2-y^2}$ orbital and the nitrogen atom orbitals. The weak distortion of the coordination polyhedron is mainly due to the *trans* III configuration adopted by the macrocycle (Fig. 5).

4. Conclusion

Three new cyclam based ligands bearing one *N*-sulfonylacamide group have been obtained, and their coordination to four different metals was studied. The replacement of the usual acetate group by an *N*-sulfonylacamide group results in a zwitterionic form of the three corresponding ligands. It has been shown that the amidate form of the pendant arm is maintained in the different complexes. In order to study competition between carboxylic and *N*-sulfonylacamide groups, novel cyclams bearing the two kinds of coordinating arms are currently synthesized in our laboratory.

Acknowledgments

This work was supported by the CNRS, the French Minister for Research, and the Regional Council of Burgundy.

Appendix A. Supplementary material

CCDC 763222, 763223, 763224, 763225 and 763226 contain the supplementary crystallographic data for L₃, CuL₃Cl, ZnL₂NO₃, CdL₃NO₃ and L₁. These data can be obtained free of charge from The Cambridge Crystallographic Data Centre via www.ccdc.cam.ac.uk/data_request/cif. Supplementary data associated with this article can be found, in the online version, at [doi:10.1016/j.ica.2011.04.013](https://doi.org/10.1016/j.ica.2011.04.013).

References

- [1] (a) R.D. Hancock, R.J. Motekaitis, J. Matshishi, I. Cukrowski, J.H. Reibenspies, A.E. Martell, *J. Chem. Soc., Perkin Trans. 2* (1996) 1925; (b) A. Bianchi, M. Micheloni, P. Paoletti, *Coord. Chem. Rev.* 110 (1991) 17; (c) E. Kimura, *Prog. Inorg. Chem.* 41 (1994) 443;

- (d) L. Fabbrizzi, M. Lichelli, P. Pallavicini, D. Sacchi, *Supramol. Chem.* 13 (2001) 659.
- [2] L. Lattuada, A. Barge, G. Cravotto, G.B. Giovenzana, L. Tei, *Chem. Soc. Rev.* 40 (2011) 3019.
- [3] (a) E. Brücher, A.D. Sherry, in: A.E. Merbach, E. Toth (Eds.), *The Chemistry of Contrast Agents in Medical Magnetic Resonance Imagings*, Wiley, New York, 2001 (Chapter 6); (b) P. Caravan, J.J. Ellison, T.J. McMurry, R.B. Lauffer, *Chem. Rev.* 99 (1999) 2293; (c) R. Delgado, V. Felix, L.M.P. Lima, D.W. Price, *Dalton Trans.* 26 (2007) 2734; (d) J.D.G. Correia, A. Paulo, P.D. Raposinho, I. Santos, *Dalton Trans.* (2011).
- [4] (a) E. Kimura, T. Koike, Y. Inouye, in: R.W. Hay, J.R. Dilworth, K.B. Nolan (Eds.), *Perspective on Bioinorganic Chemistry*, vol. 14, JAI Press, Inc., Stamford, CT, 1999, p. 145; (b) X. Liang, J.A. Parkinson, M. Weishaupl, R.O. Gould, S.L. Paisey, H.S. Park, T.M. Hunter, C.A. Blindauer, S.A. Parson, P.J. Sadler, *J. Am. Chem. Soc.* 124 (2002) 9105; (c) G.J. Bridger, R.T. Skerlj, *Advances in Antiviral Drug Design*, vol. 3, JAI Press Inc., London, UK, 1999, p. 161.
- [5] D.K. Cabbiness, D.W. Margerum, *J. Am. Chem. Soc.* 91 (1969) 6540.
- [6] E.K. Barefield, *Coord. Chem. Rev.* 254 (2010) 1607.
- [7] L. Fabbrizzi, M. Licchelli, A. Poggi, D. Sacchi, C. Zampa, *Polyhedron* 23 (2004) 373.
- [8] S. Aime, M. Botta, G. Cravotto, L. Frullano, G. Giovenzana, S. Geninatti Crich, G. Palmisano, M. Sisti, *Helv. Chim. Acta* 88 (2005) 588.
- [9] Z. Otwinowski, W. Minor, *Methods Enzymol.* 276 (1997) 307.
- [10] A. Altomare, G. Cascarano, C. Giacovazzo, A. Guagliardi, *J. Appl. Crystallogr.* 26 (1993) 343.
- [11] SHELXL97, Program for the Refinement of Crystal Structures, 1997.
- [12] F. Denat, S. Brandes, R. Guillard, *Synlett* 5 (2000) 561.
- [13] (a) V. Amendola, M. Boiocchi, L. Fabbrizzi, A. Palchetti, *Chem. Eur. J.* 11 (2005) 120; (b) B. Masereel, J. Wouters, L. Pochet, D. Lambert, *J. Med. Chem.* 41 (1998) 3239.
- [14] L. Farrugia, *J. Appl. Crystallogr.* 30 (1997) 565.
- [15] (a) M. Levitt, M.F. Perutz, *J. Mol. Biol.* 210 (1988) 751; (b) C.S. Page, H.S. Rzepa, *Electronic Conference on Trends in Organic Chemistry*, 1995.
- [16] B. Bosnich, C.K. Poon, M.L. Tobe, *Inorg. Chem.* 4 (1965) 1102.
- [17] (a) Y. Dong, S. Farquhar, K. Gloe, L.F. Lindoy, B.R. Rumbel, P. Turner, K. Wichmann, *Dalton Trans.* (2003) 1558; (b) H. Ito, T. Ito, *Acta Crystallogr., Sect. C* 41 (1985) 1598.
- [18] (a) A. Riesen, M. Zehnder, T.A. Kaden, *Acta Crystallogr., Sect. C* 47 (1991) 531; (b) I. Svobodová, P. Lubal, J. Plutnar, J. Havlíčková, J. Kotek, P. Hermann, I. Lukes, *Dalton Trans.* (2006) 5184.
- [19] (a) S. Fúzerová, J. Kotek, I. Císařová, P. Hermann, K. Binnemans, I. Lukeš, *Dalton Trans.* (2005) 2908; (b) J. Kotek, P. Lubal, P. Hermann, I. Císařová, I. Lukeš, T. Godula, I. Svobodová, P. Táborský, J. Havel, *Chem. Eur. J.* 9 (2003) 233; (c) M. Studer, A. Riesen, T.A. Kaden, *Acta Crystallogr., Sect. C* 46 (1990) 741.
- [20] (a) Y. Dong, G.A. Lawrance, L.F. Lindoy, P. Turner, *Dalton Trans.* (2003) 1567; (b) P. Comba, P. Jurisic, Y.D. Lampeka, A. Peters, A.I. Prikhod'ko, H. Pritskow, *Inorg. Chim. Acta* 99 (2001) 324.
- [21] (a) U. Sakaguchi, A.W. Addison, *J. Chem. Soc., Dalton* (1979) 600; (b) T. Murakami, T. Takei, Y. Ishikawa, *Polyhedron* 16 (1997) 89; (c) A.E. Goeta, J.A.K. Howard, D. Maffeo, H. Puschmann, J.A.G. Williams, D.S. Yufit, *J. Chem. Soc., Dalton Trans.* (2000) 1873.
- [22] (a) B.J. Hathaway, D.E. Billing, *Coord. Chem. Rev.* 5 (1970) 143; (b) J.R. Pilbrow, *Transition Ion Electron Paramagnetic Resonance*, first ed., Clarendon Press, Oxford, 1990.
- [23] C. Bucher, E. Duval, J.M. Barbe, J.-N. Verpeaux, C. Amatore, R. Guillard, *C. R. Acad. Sci. Paris Sér. II c* 3 (2000) 211.
- [24] (a) K. Miyoshi, H. Tanaka, E. Kimura, S. Tsuboyama, *Inorg. Chim. Acta* 78 (1983) 23; (b) E.V. Rybak-Akimova, A.Y. Nazarenko, L. Chen, P.W. Krieger, A.M. Herrera, V. Tarasov, P.D. Robinson, *Inorg. Chim. Acta* 324 (2001) 1.
- [25] (a) A.W. Addison, T.N. Rao, J. Reedijk, J. Van Rijn, G.C. Verschoor, *J. Chem. Soc., Dalton Trans.* (1984) 1349; (b) S. Alvarez, M. Llunell, *J. Chem. Soc., Dalton Trans.* 23 (2000) 3288.
- [26] L.E. Cheruzel, M.R. Cecil, S.E. Edison, M.S. Mashuta, M.J. Baldwin, R.M. Buchanan, *Inorg. Chem.* 45 (2006) 3191.